



Optical reflectance study of the wetting layers in (In, Ga)As self-assembled quantum dot growth on GaAs (001)

Kita, Takashi

Wada, Osamu

Nakayama, T.

Murayama, M.

(Citation)

Physical Review B, 66(19):195312-195312

(Issue Date)

2002-11-12

(Resource Type)

journal article

(Version)

Version of Record

(URL)

<https://hdl.handle.net/20.500.14094/90000119>



Optical reflectance study of the wetting layers in (In, Ga)As self-assembled quantum dot growth on GaAs (001)

Takashi Kita* and Osamu Wada

Department of Electrical and Electronics Engineering, Faculty of Engineering, Kobe University, Rokkodai 1-1, Nada, Kobe 657-8501, Japan

T. Nakayama

Department of Physics, Faculty of Science, Chiba University, 1-33 Yayoi, Inage, Chiba 263-8522, Japan

M. Murayama

Department of Electronics Engineering, The University of Electro-Communications, 1-5-1 Chofugaoka, Chofu, Tokyo 182-8585, Japan

(Received 14 November 2001; revised manuscript received 09 August 2002; published 12 November 2002)

We have studied *in situ* Stranski-Krastanov growth surface of (In,Ga)As grown by molecular-beam epitaxy on GaAs (001) using reflectance-difference (RD) spectroscopy and reflection high-energy electron diffraction. The surface of the two-dimensional wetting layer shows various structures depending on the InAs coverage and the growth temperature. At relatively low substrate temperature, the growth transition from two-dimensional to three-dimensional occurs on the (2×3) surface of (In,Ga)As, whereas at high-temperature the transition occurs on the (2×4) surface of InAs. Comparing the measured RD spectra with the calculations based on the tight-binding surface-linear-response method, we found that both $[110]$ -In and $[\bar{1}10]$ -As dimers are necessary for the (2×3) and (2×4) surfaces to explain the observed RD spectra. Time-resolved measurements demonstrate that disappearance of excess As surface triggers the islanding process. Furthermore, the In-dimer-related signal shows a redshift near the growth transition due to the strain relaxation.

DOI: 10.1103/PhysRevB.66.195312

PACS number(s): 78.66.Fd, 68.35.Bs, 71.15.Nc

I. INTRODUCTION

Self-assembled quantum dots in semiconductor heterostructures are of great interest, because of their discrete atomlike energy levels, good optical properties and promising device applications such as quantum dot laser and infrared photodetector.¹ In a lattice-mismatched system such as (In, Ga)As/GaAs, the self-assembled quantum dots can be achieved by the Stranski-Krastanov (SK) growth mode.² Above a critical thickness, the growth mode is changed from two-dimensional (2D) layer-by-layer growth to three-dimensional (3D) island growth. In the SK growth the 2D-wetting layer dramatically changes at the initial stage of the growth in order to achieve such transition from 2D to 3D growth. To control the growth mode, it is important to understand a relation between the structure of the 2D wetting layer and the transition to 3D growth. The 2D wetting layer varies as a function of the InAs coverage and the growth temperature.³ The wetting layers initially show threefold $(\times 3)$ patterns in the $[\bar{1}10]$ azimuth due to the formation of an (In,Ga)As-alloy phase.³⁻⁵ With increasing the InAs coverage, the alloy phase is followed by an InAs phase formation with the (2×4) surface reconstruction. The various possible surface conditions, which depend on growth conditions, play a key role in the SK growth mode. In this study, we performed reflectance-difference (RD) spectroscopy on the wetting layers in the SK growth of (In, Ga)As grown by molecular-beam epitaxy on GaAs (001) and simultaneously characterized the growth by reflection high-energy electron diffraction (RHEED). RD signal was measured between the complex near-normal-incidence reflectances of light linearly

polarized along two principle axes $[\bar{1}10]$ and $[110]$, which can be expressed in terms of the surface dielectric anisotropy. For optically isotropic materials, surface optical absorption contributes to the RD spectroscopy, which gives information about dynamic processes at the growth front.⁶⁻¹¹ Recently, RD spectroscopy has been used to monitor formation and development of InAs islands on GaAs(001) surface.⁸⁻¹¹ They succeeded to take RD spectra immediately after the growth of different amounts of InAs. Furthermore, time-resolved measurements at certain photon energies (especially at 4.0 eV in Ref. 10) have been carried out to study the islanding process. In this work, we focus on the wetting layer surface structure during the transition of 2D to 3D growth. We report here the observation of a new feature, negative peak near 2 eV which can be attributed to cation dimers. The surface structure near the 2D-3D growth transition is discussed.

II. EXPERIMENTS

InAs quantum dots were grown by a solid-source molecular beam epitaxy (MBE) on GaAs(001). A 120-nm-buffer layer of GaAs was grown at 530 °C. The deposition rate of InAs, estimated from homoepitaxial growths, was 1 ML/min. InAs deposition was performed at 300–480 °C. Indium desorption was apparent above 400 °C.¹² Our RD spectroscopy system is mounted on the MBE.¹¹ RD spectroscopy and RHEED measurements were carried out simultaneously under As₄ flux of about 2×10^{-6} Torr beam equivalent pressure. RD spectra were measured immediately after the deposition of InAs. For time-resolved measurements, the RD intensity fixed at a certain photon energy, and the RHEED-

spot intensity were recorded simultaneously during the InAs deposition. In this study, the transition from 2D wetting layer growth to 3D island growth is determined from the change in the RHEED pattern (picture not shown) that represents a clear signature of 2D and 3D growth.^{11,12}

RD was measured between the complex near-normal-incidence reflectances of light linearly polarized along two principle axes $[\bar{1}10]$ and $[110]$. The two-prism photoelastic-modulator configuration allows us to measure both relative amplitude $\Delta r/r$ and phase $\Delta\theta$ of the anisotropy of the complex reflectance. We converted the measured RD spectra, $\Delta r/r$ and $\Delta\theta$, into anisotropy spectra of the dielectric response $\Delta(\epsilon d)$. Here, we used the Fresnel three-phase model expressed in terms of the surface dielectric anisotropy ($\epsilon_{\bar{1}10} - \epsilon_{110}$) d .^{6,7} $\epsilon_{\bar{1}10}d$ and $\epsilon_{110}d$ are the surface dielectric responses along the $[\bar{1}10]$ and $[110]$ directions, respectively. The bulk dielectric function used in the calculation corresponding to the temperature of the measurement was obtained by data shifted according to the temperature coefficient of the critical point E_1 .

III. CALCULATION METHOD OF ANISOTROPY SPECTRA

To determine the atom positions of various reconstructed surfaces, we adopted the repeated slabs which are equivalent to fourteen atomic layers in thickness. An isolated slab consists of seven (In, Ga)As atomic layers whose bottom is terminated by hypothetical hydrogen atoms. The positions of the hydrogen atoms and the lowest three layers are fixed. The other atom positions were optimized by the *ab initio* total-energy pseudopotential method in a local density approximation (LDA), where the separable ultrasoft pseudopotential¹³ and the Ceperly-Adler exchange-correlation potential are used.¹⁴ The wave function is expanded by plane waves with the energy less than 7.3 Ry, and in the case of (1×3) surfaces the charge density is calculated by using $7 \times 20 \times 23$ mesh points in the repeated-slab unit cell and two special points in the surface Brillouin zone. Using the optimized geometries, the dielectric anisotropy was calculated by the *sp³s** tight-binding method in a surface response theory, where the slab of twenty atomic layers is used.¹⁵ The parameters of on-site and transfer energies are taken from the previous works^{16,17} and the Harrison's d^{-2} rule¹⁸ is adopted. The other details of the calculations are described elsewhere.¹⁶

IV. RESULTS AND DISCUSSION

A. RD spectra

With increasing the InAs coverage, the (1×3) , (2×3) , and (2×4) reconstructions were confirmed, depending on the InAs coverage and the growth temperature. The observed phase diagram is very similar to the diagram obtained by Belk *et al.*³ The threefold ($\times 3$) pattern in the $[\bar{1}10]$ azimuth indicates the formation of an (In, Ga)As alloy surface,³⁻⁵ and shows a so-called an asymmetric (or incommensurate) diffraction. The asymmetry in the (1×3) becomes more pro-

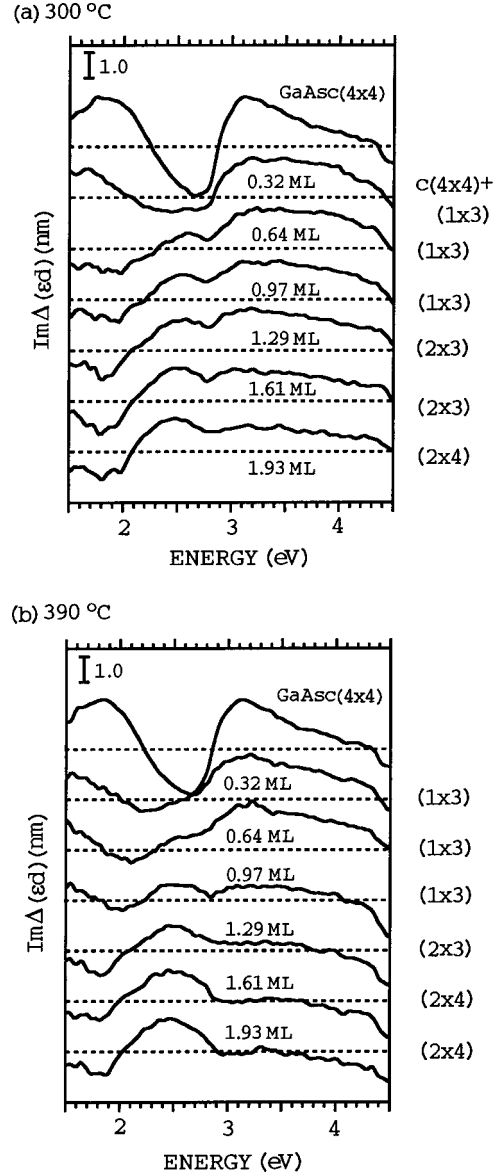


FIG. 1. Imaginary part of $\Delta(\epsilon d)$ at successive steps of InAs deposition at 300 °C (a) and 390 °C (b). The RHEED patterns are listed on the right of each spectrum.

nounced towards higher temperature. In this case, the 1/3- and 2/3-order streaks are closer together. The (2×3) surface also shows asymmetric features³ and seems to be an intermediate phase for the (2×4) surface. The 1/3- and 2/3-order streaks of the (2×3) shift outwards towards the 1/4 and 3/4 positions, respectively. At 480 °C, the RHEED pattern shows diffuse structures.³ The transition between 2D and 3D growth modes was observed on the (2×3) or (2×4) surface; at 300 °C, the growth-mode transition occurs on the (2×3) surface of (In, Ga)As, while above 350 °C the transition occurs on the (2×4) surface of InAs.

$\Delta(\epsilon d)$ spectra at successive steps of the InAs deposition at 300 and 390 °C are plotted in Fig. 1. The RHEED patterns are listed on the right of the each spectrum. Except for the structure around 3–4 eV, it seems that there is no significant difference between Figs. 1(a) and 1(b). As observed in the

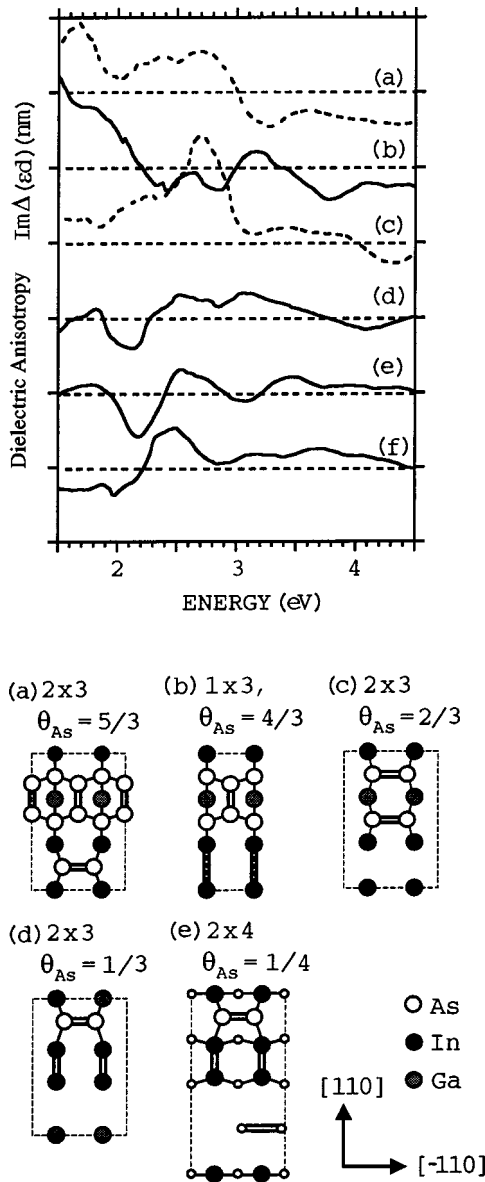


FIG. 2. Calculated imaginary part of $\Delta(\epsilon d)$ [(a)–(e)], for various (1×3) , (2×3) , and (2×4) surfaces [(a)–(e)], respectively. The spectrum (f) is the result of an InAs-bulk surface with the $(2 \times 4)\alpha 2$ structure.

previous works,^{8,10} the high-energy transitions (3–4 eV) rapidly damps with increasing the InAs coverage. This trend is remarkable at the high growth temperature. The negative signal (2.7 eV) of the initial $c(4 \times 4)$ surface is due to the optical transitions from the occupied dangling bond states to the unoccupied antibonding states of neighboring As dimers.¹⁶ With increasing the InAs coverage, the amplitude of the negative signal at 2.7 eV decreases. In addition to that, the positive signal is observed near 2.5 eV. The sign inversion observed near 2.5 eV indicates the disappearance of excess As and formation of new surfaces. At the initial stage of the growth a positive signal near 2.0 eV of the $c(4 \times 4)$ is reduced rapidly. This positive signal comes from As-As bonds between the top and second-top layers.¹⁶ Therefore, a reduction in this positive signal intensity also indicates the

desorption of excess As. On the other hand, a negative signal below 2.0 eV is observed at the high InAs coverage (>0.64 ML). Similar negative features were also observed for GaAs(001) surfaces by Kamiya *et al.*⁷ According to their results, (4×2) reconstruction obtained at a heated condition in a reduced As flux exhibits an RD spectrum that is characterized by the prominent negative feature near 2.0 eV. Based on the reported theoretical calculations, they concluded that this negative structure is assigned to the transitions between $[110]$ -Ga-dimer orbital and empty Ga lone-pair states. They also pointed out that the intermediate phase shows both set of features, the negative signal near 2.0 eV and the positive signal at 2.5 eV, because of the presence both Ga and As dimers. On the basis of the above-mentioned analysis for GaAs, we can assign the observed RD spectra of the wetting layer that also shows both set of features to the surface terminated by $[\bar{1}10]$ -As and $[110]$ -In (or Ga) dimers. The growth of the negative signal observed at the initial stage is complicated, because it correlates with the changes of the 2.5 and 2.0 eV [As(first layer)-As(second layer) bond] signals as well as the cation-dimer formation. It is noted that the surface long-range ordering keeps the (1×3) during the complication in the initial stage of the growth. Furthermore, the negative signal shows a redshift when the growth proceeds beyond the 1-ML deposition.

To explain the origin of the new $\Delta(\epsilon d)$ signals, we compared the measured data with the theoretically calculated spectra. In the calculation, we considered various (1×3) , (2×3) , and (2×4) surfaces with As dimers shown in Fig. 2. The (a) surface has a structure proposed by Sauvage-Simkin *et al.*⁵ By calculating the surface formation energies in the As-rich condition, we found that for the (1×3) and (2×3) surfaces In-Ga mixing with $\text{Ga}_{1/3}\text{In}_{2/3}$ composition is favorable to lower the strain energy caused by the lattice mismatch between InAs and GaAs.¹⁵ Moreover, considering the surface energy as a function of As-chemical potential, it is shown that the (1×3) of (b) is stable in As-rich condition whereas the (2×3) of (d) is stable in As-poor condition. The calculated $\Delta(\epsilon d)$ spectra are summarized at the top of Fig. 2, where the spectra [(a)–(e)] correspond to the surfaces [(a)–(e)] shown in the bottom part, respectively. On the other hand, the spectrum (f) is a result of an InAs-bulk surface with the $(2 \times 4)\alpha 2$ structure.¹⁹ All the calculated spectra are shifted 0.5 eV to the lower energy side because the calculations correspond to 0 K while the experiments were carried out around 700 K.

By analyzing the spectra of the (b) surface, a negative signal near 2.8 eV is attributed to the transitions from the occupied dangling-bond states of the top-layer As to the unoccupied antibonding states of $[110]$ -As dimers. A negative signal near 2.4 eV is due to the As(second layer)-cation(third layer) bonds. On the other hand, positive signals near 1.8 and 3.1 eV are related to the As(first layer)-As(second layer) bonds, respectively. For the (d), (e), and (f) surfaces, the $\Delta(\epsilon d)$ signals show a negative signal near 2 eV. This structure can be attributed to the transitions between In-dimer orbital and empty In lone-pair states. The positive signal near 2.5 eV is due to the transitions from the dangling-bond states

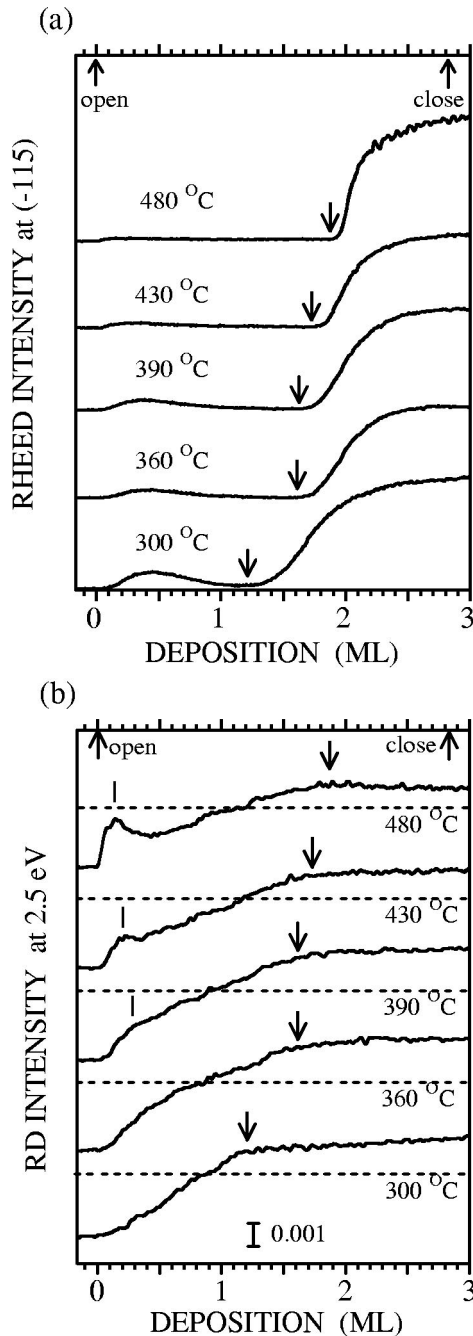


FIG. 3. Time-resolved RD $\Delta r/r$ intensity at 2.5 eV and RHEED-spot intensity at the $(\bar{1}15)$ diffraction at various growth temperatures. The arrows indicate the growth transitions.

of the top As atom to the antibonding states of the $[\bar{1}10]$ -As dimers. Since the (b) surface has high As coverage and resembles the starting $c(4 \times 4)$ GaAs surface within the surface structures considered in the present paper, we can assign the initial As-rich (1×3) surface to the (b) surface. The calculated spectrum for this surface can be compared with the spectrum obtained at the 0.32 ML deposition. At this low coverage, it is observed that the (1×3) phase is partially formed.³ From the calculation of the (b) surface, the cation-dimer bond length is increased by the mixing of cation during the growth. The calculated cation-dimer lengths with Ga,

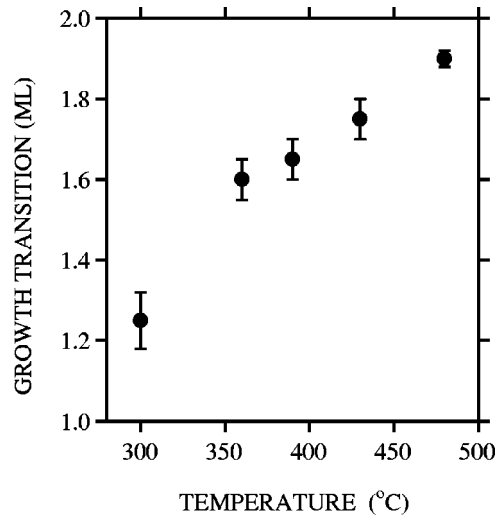


FIG. 4. Amount of deposited InAs at the growth transition as a function of growth temperature.

$\text{Ga}_{2/3}\text{In}_{1/3}$, $\text{Ga}_{1/3}\text{In}_{2/3}$, and In compositions are 2.61, 2.69, 2.84, and 2.86 Å, respectively. In the previous work observed by using scanning tunneling microscopy,³ the variation of the indium content across the surface was reported. According to their observations, the indium concentration in the third layer increases as the diffraction pattern becomes more symmetric towards the lower temperature and the higher InAs coverages. These results support the cation mixing effects. The negative (near 2.0 eV) and positive (2.5 eV) signals observed at the surfaces with ≥ 1 ML InAs can be reproduced by the spectra for the (d), (e), and (f) surfaces. The RD spectrum at the 1.93-ML deposition in Fig. 1 agrees well with the calculated spectra for the (f) surface. Our calculated result for the InAs-bulk surface also agrees well with the recently reported spectra.^{20,21} The fact that the agreement with these experiments is good shows the validity of our calculations. However, the E_1 and $E_1 + \Delta_1$ bulk critical points are close to the positive signal at 2.5 eV. In a recent *ab initio* DFT-LDA study for (2×4) GaAs(001), it is pointed out that the RD feature associated to As dimers by tight binding results appears to be bulk related.²² Recently, Berkovits²⁰ and Goletti²¹ interpreted that a high-energy flank of the positive broad peak near 2.5 eV would coincide with the bulk critical points. Thus, the origin of this positive signal is not fully understood at this moment. However, as reported in the previous papers,^{20,21} it is reasonable to consider that the unresolved broad feature near 2.5 eV relates to the As dimer and the bulk critical points.

According to the above-mentioned assignment for the RD signals, it is considered that the complicated redshift (from 2.3 to 1.8 eV) of the negative signal in the (1×3) phase is caused by evolution of (1) the positive signal near 2.5 eV, (2) the 2.0 eV signal from the As(first layer)-As(second layer) bonds, (3) the negative signal from As(second layer)-cation(third layer) bonds, and (4) the negative signal from In dimers. The positive signal near 2.5 eV seems to show a redshift with increasing the InAs coverages. The calculated As-dimer length for the (b), (d), and (e) surfaces are 2.42, 2.55, and 2.49 Å, respectively. This theoretical result does

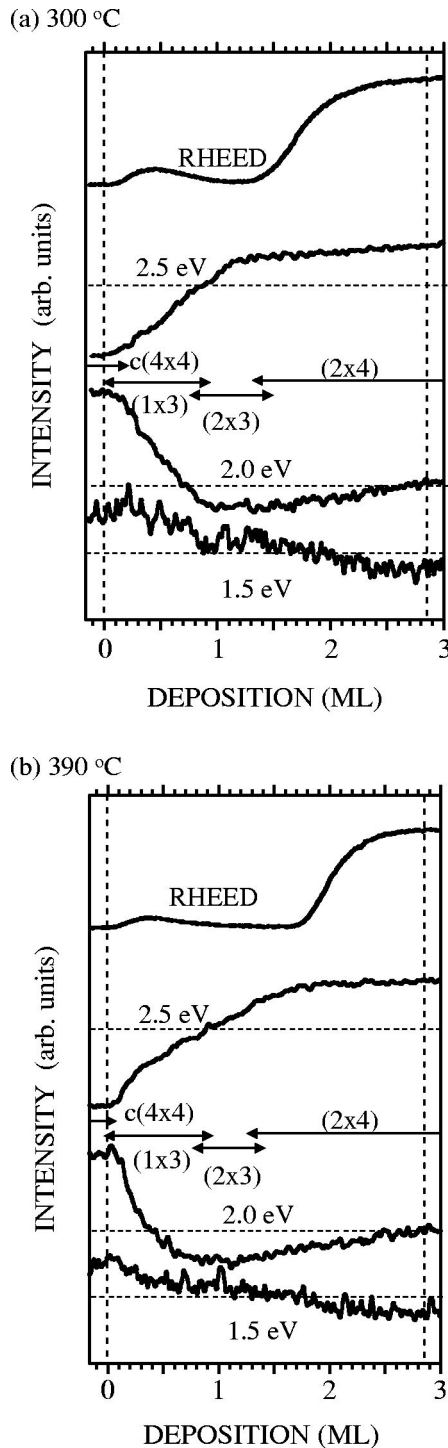


FIG. 5. Time-resolved RD intensity is taken at 1.5 and 2.0 eV at 300 °C (a) and 390 °C (b) compared with the RHEED-spot intensity at the $(\bar{1}15)$ diffraction and RD intensity at 2.5 eV. Observed RHEED patterns are also shown.

not interpret the energy shift. Thus, the energy shift would be caused by the complicated redshift of the negative signal.

The results presented here reveal the variety of the short-range order of the (1×3) phase. The cation mixing may cause such variations. But, the peculiar properties of the (1×3) surface is not clear in detail. Considering that the As

coverage decreases with changing the surface from (a) to (f), we can expect that the initial (1×3) surface approaches the surface (f) through the (d) ($\theta_{As}=1/3$) and (e) ($\theta_{As}=1/4$) surfaces toward higher InAs coverages.

B. Time-resolved observation of RD signal

The RD spectra were measured immediately after the deposition of InAs. However, the growth surface does not keep the same structure during the measurement. Actually, the RD spectrum proceeds slightly the structure with respect to the time interval between the measurements. We measured time-resolved RD intensity $\Delta r/r$ at different photon energies. Time-resolved RD intensity at 2.5 eV and the RHEED-spot intensity at the $(\bar{1}15)$ diffraction are plotted in Fig. 3 for various growth temperatures. The RHEED-spot intensity increases when islands are formed. Arrows indicate the growth transition. Figure 4 shows the amount of the deposited InAs at the growth transition as a function of the growth temperature. With increasing the growth temperature, the amount of the deposited InAs at the growth transition becomes increased, and the increase of the diffraction intensity becomes steeper, i.e., islands are formed rapidly, when the nucleation is initiated. Indium desorption being apparent above 400 °C causes a further increase of the amount of the deposited InAs.

The RD signal at 2.5 eV shows the sign inversion and the intensity converges to a constant positive level for the $(2 \times 4)\alpha_2$. It is noted that the positive signal starts to saturate at the growth transition.⁸⁻¹⁰ This means that the disappearance of the excess As surface triggers the islanding process. At the zero cross time of the RD signal, the negative signal from the $[110]$ -As dimer in the (1×3) surface balances with the positive one from the $[\bar{1}10]$ -As dimer of the (2×3) . With increasing the growth temperature, a rapid decrease of the surface anisotropy is observed just after the InAs growth. This feature is indicated by solid bars in Fig. 3(b), at which the RHEED pattern of the $c(4 \times 4)$ completely disappears, and the further deposition results in the formation of the asymmetric (1×3) . This corresponds to the commensurate and incommensurate transition that can appear when multiplication of faulted sequences takes place in a periodic stacking.^{3,5}

RD intensities taken at 1.5 and 2.0 eV are shown in Fig. 5 together with the RHEED-spot intensity. The 2.0-eV signal comes from the As(first layer)-As(second layer) bond. At 390 °C, the 2.0 and 2.5 eV signals change rapidly just after the InAs growth because of desorption of the excess As, whereas the changes at 300 °C is almost linear. During the (2×3) surface, the 1.5 and 2.0 eV signals do not show significant changes. After that, the (2×4) surface appears and the 1.5 eV signal starts to decrease. In corresponding with this change, the 2.0 eV signal starts to increase. The redshift of the negative signal as observed in Fig. 1 causes these results. Especially, it is thought that the energy shift of the negative signal observed beyond the 1-ML deposition is caused by relaxation of the misfit strain. The 1.5-eV signal intensity stops decreasing its intensity after finishing the islanding. This result is consistent with the macroscopic study

of the SK process²³ in which the strain relaxation plays a key role in self-limiting properties of the islanding.

V. CONCLUSIONS

We studied the wetting layer surface during the SK growth of (In, Ga)As on GaAs(001) by RD spectroscopy. A quite small amount of InAs deposition changes the surface structure from the initial As-rich $c(4\times4)$ of GaAs to the (1×3) of (In, Ga)As. The (1×3) surface shows various RD spectra with increasing the InAs coverage. After that, the (2×3) surface appears and is followed by the (2×4) surface. The surface structures of wetting layer were studied by comparing the observed $\Delta(\epsilon d)$ spectra obtained at various InAs coverages with the calculations of the various surfaces by the tight-binding surface-linear-response method. We found that both In and As dimers are necessary to explain the observed spectra. Time-resolved observation of the RD intensity shows that (1) the 2.5-eV signal starts converging to a

constant level at the growth transition and that (2) the 1.5-eV signal ([110]-In dimer) stops decreasing after finishing the islanding. These results suggest that the islanding is triggered by the desorption of excess-As atoms and stopped by the relaxation of the misfit strain.

ACKNOWLEDGMENTS

The authors acknowledge K. Yamashita, Kobe University, and I. Kamiya, Mitsubishi Chemical Corporation, and K. Shiraishi, Tsukuba University, for their useful discussions. One of the authors (T.K.) thanks T. Nishino, Kobe City College of Technology, and H. Nakayama, Osaka City University, for their continuous encouragement during this work. This work was supported by the Venture Business Laboratory Project of the Graduate School of Science and Technology at Kobe University and in part by the Scientific Research Grant-in-Aid from the Ministry of Education, Culture, Sports, Science and Technology.

*Also at Venture Business Laboratory, Kobe University. Electronic address: kita@eedept.kobe-u.ac.jp

¹D. Bimberg, M. Grundmann, and N. N. Ledentsov, *Quantum Dot Heterostructures* (Wiley, New York, 1998), and references therein.

²F. Houzay, C. Guille, J.M. Moison, P. Henoc, and F. Barthe, J. Cryst. Growth **81**, 67 (1987).

³J.G. Belk, C.F. McConvill, J.L. Sudijono, T.S. Jones, and B.A. Joyce, Surf. Sci. **387**, 213 (1997).

⁴J.G. Belk, J.L. Sudijono, D.M. Holmes, C.F. McConvill, T.S. Jones, and B.A. Joyce, Surf. Sci. **365**, 735 (1996).

⁵M. Sauvage-Simkin, Y. Garreau, R. Pinchaux, and M.B. Véron, Phys. Rev. Lett. **75**, 3485 (1995).

⁶J.D.E. McIntyre and D.E. Aspnes, Surf. Sci. **24**, 417 (1971).

⁷I. Kamiya, D.E. Aspnes, L.T. Florez, and J.P. Harbison, Phys. Rev. B **46**, 15 894 (1992).

⁸E. Steimentz, J.-T. Zetter, W. Richiter, D.I. Westwood, D.A. Woolf, and Z. Sobiesierski, J. Vac. Sci. Technol. B **14**, 3058 (1996).

⁹E. Steimentz, F. Schienle, J.-T. Zetter, W. Richiter, D. I. Westwood, Z. Sobiesierski, C. Matthai, B. Junno, M. Miller, and L. Samuelson (unpublished).

¹⁰D.I. Westwood, Z. Sobiesierski, C.C. Matthai, E. Steimentz, J.-T. Zetter, and W. Richiter, J. Vac. Sci. Technol. B **16**, 2358 (1998), and references therein.

¹¹T. Kita, K. Yamashita, H. Tango, and T. Nishino, Physica E (Amsterdam) **7**, 891 (2000).

¹²T. Kita, K. Tachikawa, H. Tango K. Yamashita, and T. Nishino, Appl. Surf. Sci. **159**, 503 (2000).

¹³K. Shiraishi, Thin Solid Films **272**, 345 (1996).

¹⁴J.P. Perdew and A. Zunger, Phys. Rev. B **23**, 5048 (1981).

¹⁵T. Nakayama and M. Murayama (unpublished).

¹⁶M. Murayama, K. Shiraishi, and T. Nakayama, Jpn. J. Appl. Phys. **37**, 4109 (1998).

¹⁷P. Vogl, H.P. Hjalmarson, and J.D. Dow, J. Phys. Chem. Solids **44**, 365 (1983).

¹⁸W. A. Harrison, *Electronic Structure and the Properties of Solids, The Physics of the Chemical Bonds* (Freeman, San Francisco, 1980).

¹⁹H. Yamaguchi and Y. Horikoshi, Phys. Rev. B **95**, 9836 (1995).

²⁰V.L. Berkovits, N. Witkowski, Y. Borensztein, and D. Paget, Phys. Rev. B **63**, 121214 (2001).

²¹C. Goletti, F. Arciprete, S. Almaguira, P. Chiaradis, N. Esser, and W. Richter, Phys. Rev. B **64**, 193301 (2001).

²²W.G. Schmidt, F. Bechstedt, K. Fleischer, C. Cobet, N. Nsner, W. Richter, J. Bernholc, and G. Onida, Phys. Status Solidi A **188**, 1401 (2001).

²³K. Okajima, K. Takeda, N. Oyama, K. Shiraishi, and T. Ohno, Jpn. J. Appl. Phys. **39**, L917 (2000).